RESEARCH ARTICLE   OPEN ACCESS

Periodic material-based vibration isolation for satellites

Xinnan Liu[1], WitartoWitarto[2], Xin Nie[3], Zhifei Shi[1] andY. L. Mo[2]

[1]School of Civil Engineering, Beijing Jiaotong University, Beijing 100044, China
[2]Department of Civil and Environmental Engineering, University of Houston, TX 77004, USA
[3]Department of Civil Engineering, Tsinghua University, Beijing 100084, China

Abstract
The vibration environment of a satellite is very severe during launch. Isolating the satellitevibrations during launch will significantly enhance reliability and lifespan, and reduce the weight of satellite structure and manufacturing cost. Guided by the recent advances in solid-state physics research, a new type of satellite vibration isolator is proposed by usingperiodic material that is hence called periodic isolator. The periodic isolator possesses a unique dynamic property, i.e., frequency band gaps. External vibrations with frequencies falling in the frequency band gaps of the periodic isolator are to be isolated. Using the elastodynamics and the Bloch-Floquet theorem, the frequency band gaps of periodic isolators are determined. A parametric study is conducted to provide guidelines for the design of periodic isolators. Based on these analytical results, a finite element model of a micro-satellite with a set of designed periodic isolators is built to show the feasibility of vibration isolation. The periodic isolator is found to be a multi-directional isolator that provides vibration isolation in the three directions.

Keywords: vibration isolation; periodic isolator; frequency band gaps

I. Introduction

The vibration environment of a satellite is very severe during launch. The exhaust steams of the engines and solid rocket boosters will produce vibrations transmitted to the satellite through the launch vehicle, which may cause severe consequences, such as fatigue and failure of satellites[1,2]. Various methods have been proposed to suppress or isolate the vibration transmitted to the satellites, including passive vibration isolation and active vibration isolation[3-7].

Recently, research in the field of solid-state physics shows that periodic composite structures, which consist of different materials arranged in a periodic manner in space, exhibits a unique dynamic property, called frequency band gaps. When wave frequency fall in the frequency band gaps of the periodic structure, the wave will be filtered out through the periodic structure[8-11].With inspiration by the concept of band gaps, periodic foundations are proposed for seismic isolation in civil engineering field[12,13]. The periodic foundations are arranged periodically in one, two, and threedirections, which are defined as one-dimensional periodicfoundation (1D), two-dimensional periodic foundation (2D),and three-dimensional periodic foundation (3D), respectively. Xiang *et al.*[14] both theoretically and experimentally validated the feasibility of the 1D periodic foundation made of alternating concrete and rubber layers. The shaking table experimental results show that the 1D periodic foundation can effectively filter out the waves with frequencies in its band gap.Subsequently, Yan *el al.*[15,16] conducted free field tests to study the 2D and 3D periodic foundations. The test results show the 2D periodic foundation caneffectively reduce the response of the upper structure forexcitations within the frequency band gaps.All these experimental results enhance the feasibility of application of periodicstructures in vibration isolation.

In this paper, periodic material-based vibration isolators for satellitesare proposed, which are called periodic isolatorsfrom hereafter.A parametric study is conducted to provide guidelines for the design of periodic isolators. With proper design, frequency band gaps of the periodic isolator will cover mainfrequency range of vibrations that the satellite is subjected to.The feasibility of vibration isolation by the designed periodic isolators is validated by the dynamic response analysis of a micro-satellite with a set of periodic isolators.

II. Basic theory

To demonstrate how the mechanism of frequency band gaps works, two alternating layers of different isotropic materials are arranged as shown in Fig. 1(a). For the coordinate system specified, any two adjacent layers in the body comprise a unit cell, and this unit cell is completely invariant under a lattice translation along the *z*-direction. Each layer is assumed to be infinitely extended in the plane. The thickness of the layer A and the layer B of a unit cell is h_1 and h_2, respectively. The periodicity of the isolator makes it possible to investigate the frequency band gaps by studying one unit cell, as shown in Fig. 1(b).

Let v, w be displacements in the y- and z-direction, respectively. Consider an elastic wave with propagation along the z-direction. The equation of motion in each layer is given by

$$\frac{\partial^2 u_i}{\partial t^2} = C_i^2 \frac{\partial^2 u_i}{\partial z_i^2}, \tag{1}$$

where $u=w$ and $C = C_p = \sqrt{(\lambda + 2\mu)/\rho}$ for longitudinal wave (P wave), or $u=v$ and $C = C_t = \sqrt{\mu/\rho}$ for transverse wave (S wave). The coefficients λ and μ are Lamé's elastic constants, and ρ is density. The index $i=1, 2$ indicates layers A and B, respectively. For the free vibration analysis, a plane wave form solution to Eq.(1) is assumed

$$u_i(z_i,t) = Ue^{i(k\cdot z_i - \omega \cdot t)} = u_i(z_i)e^{-i\omega\cdot t}, \tag{2}$$

where k is the wave number and ω the angular frequency. Substituting Eq.(2) into Eq.(1) yields

$$C_i^2 \frac{\partial^2 u_i(z_i)}{\partial z_i^2} + \omega^2 u_i(z_i) = 0. \tag{3}$$

The general solution of this equation is found as follows:

$$u_i(z_i) = A_i \sin(\omega z_i / C_i) + B_i \cos(\omega z_i / C_i). \tag{4}$$

$$\begin{bmatrix} \sin(\omega h_1/C_{t1}) & \cos(\omega h_1/C_{t1}) & 0 & -1 \\ \mu_1 C_{t2}\cos(\omega h_1/C_{t1}) & -\mu_1 C_{t2}\sin(\omega h_1/C_{t1}) & -\mu_2 C_{t1} & 0 \\ 0 & e^{ik\cdot h} & -\sin(\omega h_2/C_{t2}) & -\cos(\omega h_2/C_{t2}) \\ \mu_1 C_{t2}\cdot e^{ik\cdot h} & 0 & -\mu_2 C_{t1}\cos(\omega h_2/C_{t2}) & \mu_2 C_{t1}\sin(\omega h_2/C_{t2}) \end{bmatrix} \begin{bmatrix} A_1 \\ B_1 \\ A_2 \\ B_2 \end{bmatrix} = 0. \tag{8}$$

There are four unknown constants A_1, A_2, B_1 and B_2 which are determined by boundary and continuity conditions. For the case of transverse waves, the normal stress σ_z in each layer is zero which automatically satisfies the continuous condition at the interface. The stress continuity across the interface requires that the shear stress τ is continuous. Therefore, the continuity of displacement and stress at the interface $z_2 = 0$ (or $z_1 = h_1$) are

$$u_1(h_1) = u_2(0), \quad \tau_1(h_1) = \tau_2(0). \tag{5}$$

Due to the periodicity in the z-direction, according to the Bloch-Floquet theorem, the displacement and stress must satisfy the following periodic boundary conditions

$$u_1(0)e^{ik\cdot h} = u_2(h_2), \quad \tau_1(0)e^{ik\cdot h} = \tau_2(h_2), \tag{6}$$

where $i = \sqrt{-1}$ and $h = h_1 + h_2$. The shear stress can be expressed as

$$\tau_i(z_i) = \mu_i \partial u_i / \partial z_i = \mu_i \omega \left[A_i \cos(\omega z_i / C_{ti}) - B_i \sin(\omega z_i / C_{ti}) \right] / C_{ti}. \tag{7}$$

Substituting Eqs.(4) and (7) into Eqs.(5) and (6), we have

A necessary and sufficient condition for the existence of a non-trivial solution to Eq. (8) is that the determinant of the coefficient matrix is zero. After the expanding the determinant, one obtains the dispersion relation for ω as a function of k which is given by

$$\cos(k\cdot h) = \cos\left(\frac{\omega h_1}{C_{t1}}\right)\cos\left(\frac{\omega h_2}{C_{t2}}\right) - \frac{1}{2}\left(\frac{\rho_1 C_{t1}}{\rho_2 C_{t2}} + \frac{\rho_2 C_{t2}}{\rho_1 C_{t1}}\right)\sin\left(\frac{\omega h_1}{C_{t1}}\right)\sin\left(\frac{\omega h_2}{C_{t2}}\right). \tag{9}$$

Because $|\cos(k\cdot h)| \leq 1$, Eq.(9) is satisfied only when the value of the right-hand side is between -1 and +1. The band gaps are the values of ω and k that are the solutions to Eq.(9) but fall outside the range of -1 to 1. Following the same procedure, one can derive a similar result for the case of longitudinal waves. If materials A and B are the same, i.e., $C_{t1} = C_{t2} = C_t$ and $\rho_1 = \rho_2$, we get the dispersion relation for a homogenous material as $\cos(k\cdot h) = \cos(\omega h/C_t)$ where $\omega = kC_t$. For any value of k, we can find a frequency ω to satisfy this relation. This is why there are no band gaps in a homogenous material.

Though the wave number k is unrestricted, it is only necessary to consider k limited to the first Brillouin zone, i.e., $k \in [-\pi/h, \pi/h]$. In fact, if we choose a wave number k_0 different from the original k in the first Brillouin zone by a reciprocal lattice vector, for example $k_0 = k + 2n\pi/h$ where n is an integer,

we may obtain the same set of equations because of the exponential $e^{ik_0 h} = e^{ik\cdot h}$ in Eq.(8). As an example, two common materials in satellites, Al 6061-T6 and rubber, whose material properties as listed in Table 1, are used to fabricate the periodic isolator. The thickness of the Al 6061-T6 and rubber layers are h_1=7.2mm and h_2=4.8mm, respectively. Fig. 2 presents the variations of frequencies ω for both transverse wave and longitudinal wave as a function of the reduced wave number k in the first Brillouin zone. The introduction of periodicity implies the opening of gaps at $k=0$ or $k=\pm\pi/h$, as shown by the shaded area in Fig. 2. For transverse wave, the first four band gaps are: 214.1Hz-625.2Hz, 697.3Hz-1250.3Hz, 1289.6Hz-1875.6Hz and 1902.3Hz-2500.0Hz. For longitudinal modes, the first band gap starts from 815.6Hz to 2381.6Hz. It is also seen that the maximum attenuation coefficient in a band gap is observed at the center frequency of it.

III.   Proof-of-concept study

Based on the theoretical study of the frequency band gaps, an experimental study was conducted to investigate the feasibility of a 1D periodic foundation. A small-scale model frame on a periodic foundation was designed, fabricated, and tested using the shake table facility at the laboratory of the international collaborator[11]. As shown in Fig.3, specimen A is a steel frame fixed on the shake table. Specimen B is a steel frame of the same design as specimen A but is fixed on a 1D periodic foundation. The concrete layers and rubber layers are bonded together by polyurethane (PU) glue for which the anti-pull strength is larger than 1 MPa, and the tear strength is larger than 6 MPa. Displacements of the specimens were recorded by Linear Variable Differential Transformers (LVDTs). The 1975 Oroville seismogram obtained from the PEER Ground Database was used as the input motion for the shake table tests. The nominal peak ground acceleration (PGA) is scaled to 0.046g. Fig. 4 shows the displacement time histories of the top of the frames. For the frame on a periodic foundation, the peak horizontal displacement is reduced by as much as 60% as compared to that of the frame without a periodic foundation. These preliminary test results are promising and support the feasibility of periodic material-based vibration isolators for satellites.

IV.   Parametric study

The effects of the periodic constant (i.e., the thickness of the unit cell) and the filling fraction of rubber (i.e., the volume fraction of the rubber layer) are investigated. Both the band gaps of longitudinal waves and shear waves come to lower frequencies as the periodic constant increases, as shown in Fig. 5 where the filling ratio of rubber is fixed as 0.5. Moreover, the width of these band gaps decrease consistently with the increase of the periodic constant.

Fig. 6 shows the band gaps of longitudinal waves and shear waves changing with the filling ratio of rubber. It is found that the UBF decreases with the increase of the filling ratio. The key result of this effort will be to obtain the design of a periodic support that possesses both low and wide frequency band gaps that will make its use appropriate for the design of satellites. Based on the results, the most appropriate periodic isolators can be designed for practical application.

V.   Satellite with periodic isolators

The results in Section 4 can provide a basic concept for a periodic isolation for satellites. The analytical results obtained from Section 4 are based on the assumption that the unit cells of the periodic isolator are infinite in the periodicity direction.

However, the periodic isolator is with finite unit cells in practical application. In this section, as shown in Fig. 7, an ANSYS model is built for a micro-satellite system with periodic isolators according to the results from above sections, where the satellite is fixed on the periodic isolators. The thickness of the Al 6061-T6 and rubber layers areh_1=7.2mm and h_2=4.8mm, respectively. A 3-layer periodic isolator (Al-rubber-Al) and a 5-layer periodic isolator (Al-rubber-Al-rubber-Al) are considered, as shown in Fig. 7.

5.1.   frequency-domain response under longitudinal waves

The scanning frequency analysis is conducted to verify the feasibility of the periodicisolators in vibration isolation.A harmonic excitation with amplitude δ_z is applied to the bottom of the isolators. The other two DOFs in the *x*- and *y*-directions are fixed when the amplitude δ_z is applied in the *z*-direction. The frequency of the excitation is increased from 0.1 to 2000.1 Hz with an interval Δf = 2.5 Hz. Displacement responses of the reference nodesN1 and N10are collected. The scanning frequency studygives the frequency response functions (FRFs) of the reference points with periodic isolators and without periodic isolators.The FRF is defined as $20\log(\delta_o / \delta_z)$ where δ_0 is the amplitude of displacement of the reference nodes. Note that if the input displacement and the output displacement are the same then the log value is 0. Therefore, a negative number in FRF indicates an effective isolation. Fig. 8gives acomparison of each of both the node N1 and N10 responsesbetween the FRFs of the satellite with the periodic isolators and without isolators. It can be seen that the FRFs of the satellite with periodic isolators are drastically reduced, when compared to that without isolators. The maximum attenuation exceeds 75dB for the 3-layer periodic isolator, which means more than 90% of the vibration with the corresponding frequency is reduced. Moreover, the more unit cells are used, the stronger attenuation can be achieved, as shown in Fig. 8.

5.2.   frequency-domain response under shear waves

A harmonic excitation with amplitude $\delta_i\ (i = x,\ y)$is applied to the bottom of the isolators. The other two DOFs are fixed when the amplitude δ_i is applied in the *i*-direction.Figs. 9and 10 present the FRFs of the satellite under excitation in the *x*-direction and *y*-direction, respectively. It can be seen that the FRFs of the satellite with periodic isolators are drastically reduced compared to that without isolators. Apparently, the periodic isolators greatly reduce the dynamic responses of the satellite under shear waves. Thus, the proposed periodic isolator can

serve as a multi-directional isolator for satellites by isolating damagingwaves in three directions.

5.3. time-domain response under harmonic excitations

In this subsection, time-domain dynamic responses of the satellite with periodic isolators are studied. Considering an harmonic displacement excitation at the bottom of the periodic isolators, the time history is given as $u_i = \sin(2\pi \cdot f \cdot t)$ (mm), $i=x$, y, z. the excitation frequency is taken as f=1000Hz, which is inside both the band gaps for longitudinal waves and shear waves.Fig. 11(a) shows the dynamic response of node N10 under the harmonic excitation in the x-direction. It can be seen that the response of the satellite with periodic isolator is much smaller than that without isolators. Similar results can also be found for the excitation in y- and z-direction, as shown in Fig. 11(b) and (c), which verifies again that the periodic isolators can serve as multi-directional isolators.

VI. Conclusions

Periodic material-based vibration isolators for satellites are proposed. Based on the elastodynamics, the frequency band gaps are determined. With proper design, the frequency band gaps can cover the main frequency range of vibrations that the satellite is subjected to during launch. The finite element analysis of a micro-satellite with a set of designed periodic isolators is also conducted in the paper.The results show that the periodic isolator serves a multi-directional isolator when the excitation frequency falls in its band gaps.

VII. Acknowledgments

References

[1] Chen Y, Fang B, Yang TZ, Huang WH. Study of Whole-spacecraft Vibration Isolators Based on Reliability Method. Chinese Journal of Aeronautics 2009;22 (2):153-9.

[2] Wijker JJ. Spacecraft structures. Springer Science & Business Media; 2008.

[3] Zhang YW, Fang B, Zang J. Dynamic features of passive whole-spacecraft vibration isolation platform based on non-probabilistic reliability. J Vib Control 2015;21 (1):60-7.

[4] Omidi E, Mahmoodi SN, Shepard WS. Vibration reduction in aerospace structures via an optimized modified positive velocity feedback control. Aerospace Science and Technology 2015;45:408-15.

[5] Liu C, Jing XJ, Li FM. Vibration isolation using a hybrid lever-type isolation system with an X-shape supporting structure. Int J Mech Sci 2015;98:169-77.

[6] Winthrop MF, Cobb RG, Survey of state-of-the-art vibration isolation research and technology for space applications, in: Smart Structures and Materials 2003: Damping and Isolation, San Diego, 2003, pp. 13-26.

[7] Bicos AS, Johnson C, Davis LP, Need for and benefits of launch vibration isolation, in: Smart Structures and Materials 1997: Passive Damping and Isolation, San Diego, 1997, pp. 14-9.

[8] Thomas EL, Gorishnyy T, Maldovan M. Phononics: Colloidal crystals go hypersonic. Nat Mater 2006;5 (10):773-4.

[9] Kaur G, Sappal AS, Singh H.Band Gap Computation of Two Dimensional Photonic Crystal for High Index Contrast Grating Application. Int'l Journal of Engineering Research and Applications. 2014;4 (5):136-9.

[10] Joe YS, Essiben JF, Hedin ER. Surface-Wave Suppression Using Periodic Structures. Int'l Journal of Engineering Research and Applications. 2013;3 (2):1562-6.

[11] Ghasemi MA, Khodadadi R, Banaei HA. Design and simulation of all optical multiplexer based on one-dimensional photonic crystal for optical communications systems. Int'l Journal of Engineering Research and Applications. 2012;2(6):960-8.

[12] Liu XN, Shi ZF, Xiang HJ, Mo YL. Attenuation zones of periodic pile barriers with initial stress. Soil Dyn Earthq Eng 2015;77:381-90.

[13] Jia GF, Shi ZF. A new seismic isolation system and its feasibility study. Earthq Eng Eng Vib 2010;9 (1):75-82.

[14] Xiang HJ, Shi ZF, Wang SJ, Mo YL. Periodic materials-based vibration attenuation in layered foundations: experimental validation. Smart Mater Struct 2012;21 (11):112003.

[15] Yan Y, Cheng Z, Menq F, Mo YL, Tang Y, Shi Z. Three dimensional periodic foundations for base seismic isolation. Smart Mater Struct 2015;24 (7):075006.

[16] Yan Y, Laskar A, Cheng Z, Menq F, Tang Y, Mo YL, Shi Z. Seismic isolation of two dimensional periodic foundations. J Appl Phys 2014;116 (4):044908.

Tables
Table 1. Material parameters

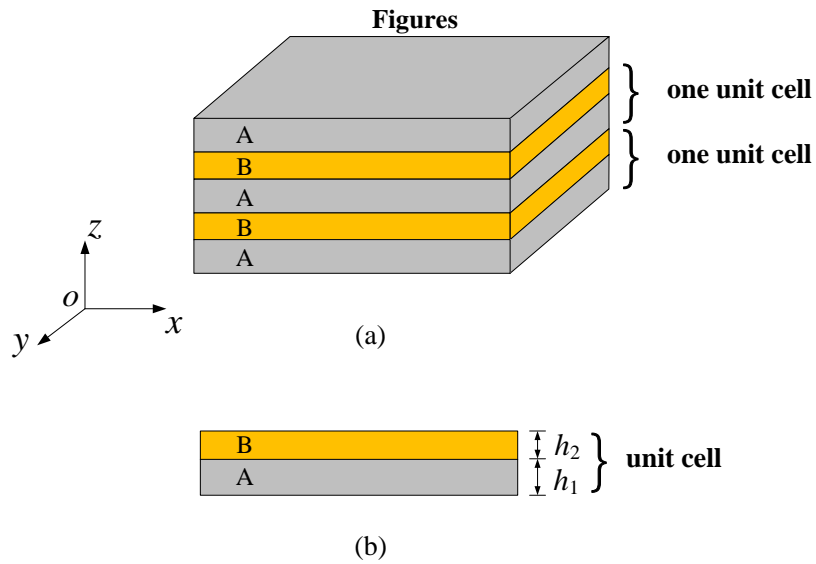| Materials	Mass density(kg/m^3)	Young's modulus (GPa)	Poisson's ratio
Al 6061-T6	2700	68.9	0.33
Rubber	1300	1.47×10^{-4}	0.46

Figures

(a)

(b)

Fig. 1.Configuration of a periodic isolator and its unit cell.

(a)   (b)
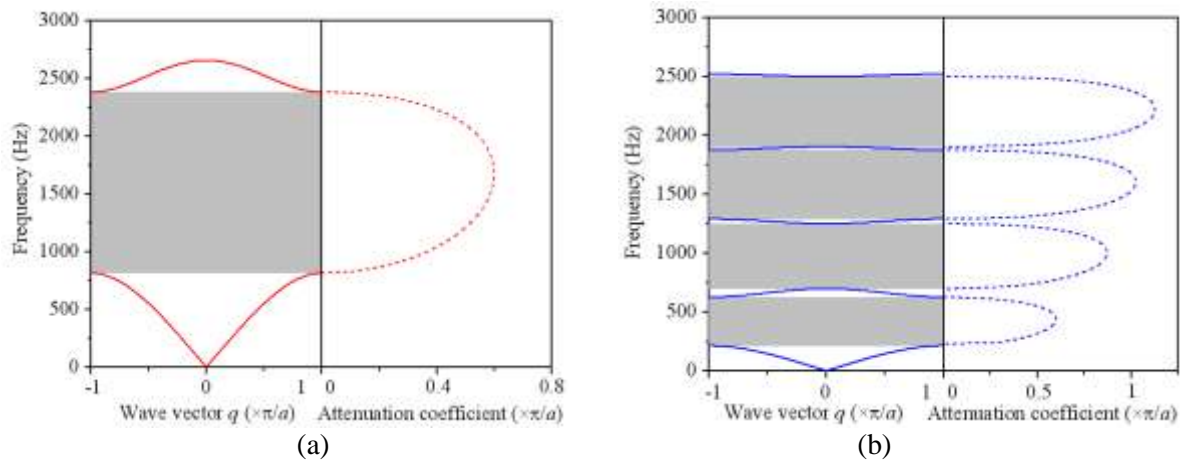
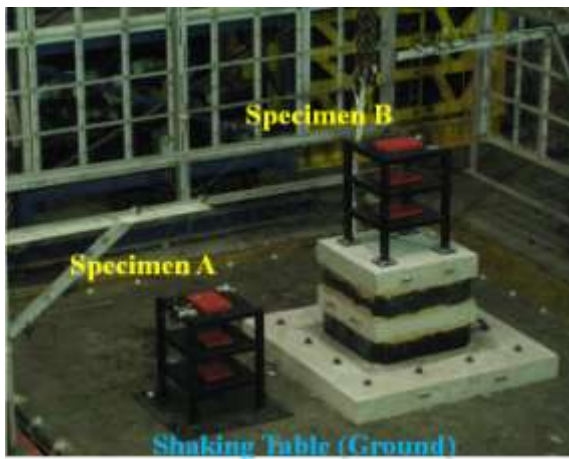**Fig. 1.** Dispersion curves for (a) longitudinal waves and (b) shear waves in a periodic isolator.

Fig. 3. Test setup for specimens A (without periodic foundation) and B (with periodic foundation).
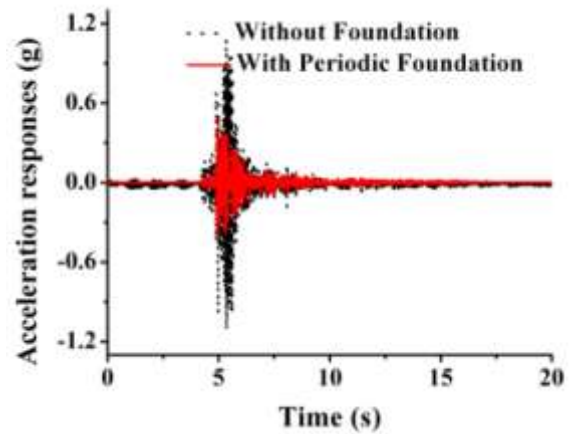
Fig. 4. Acceleration on the top of the frames.
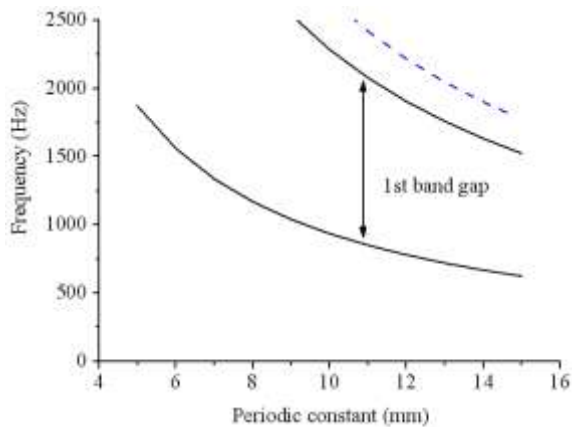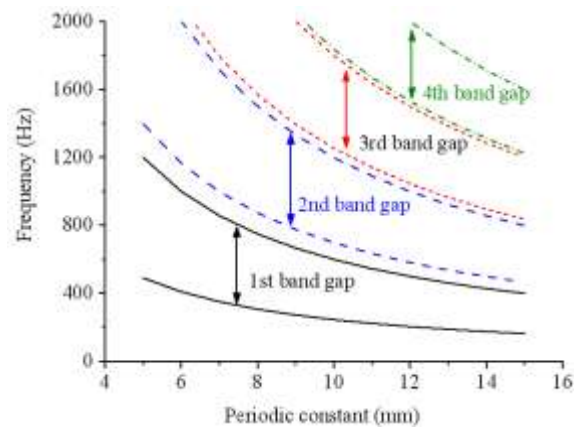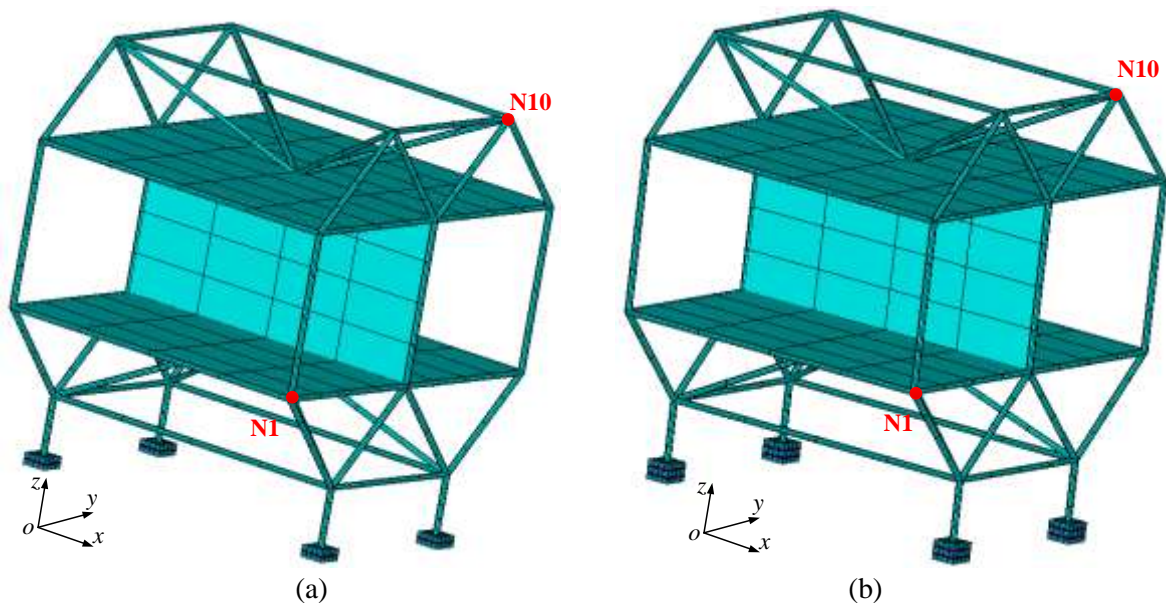

(a)   (b)

Fig. 5. Band gaps of (a) longitudinal waves and (b) shear waves versus the periodic constant.

(a)   (b)

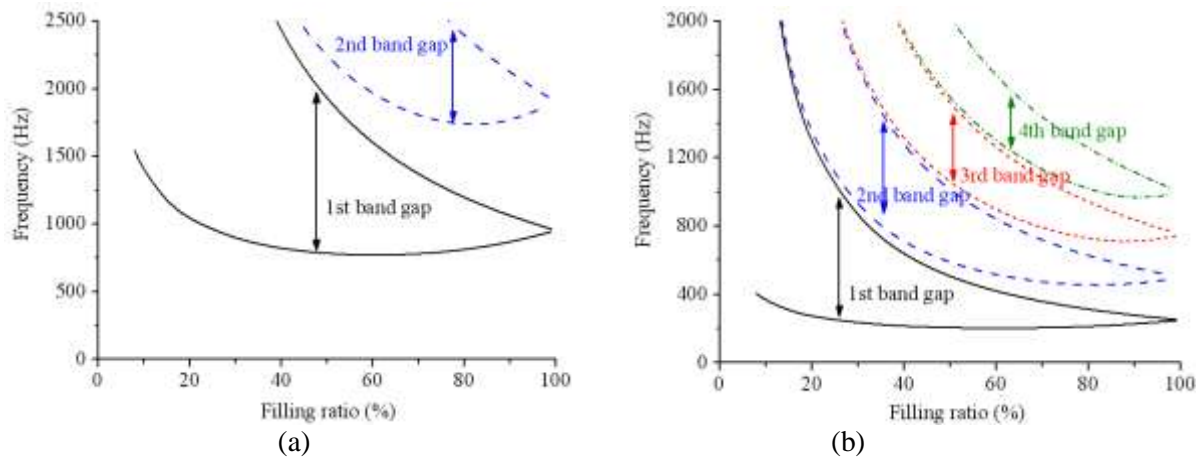**Fig. 7.** A satellite with (a) 3-layer periodic isolator and (b) 5-layer periodic isolator.

| (a) | (b) |

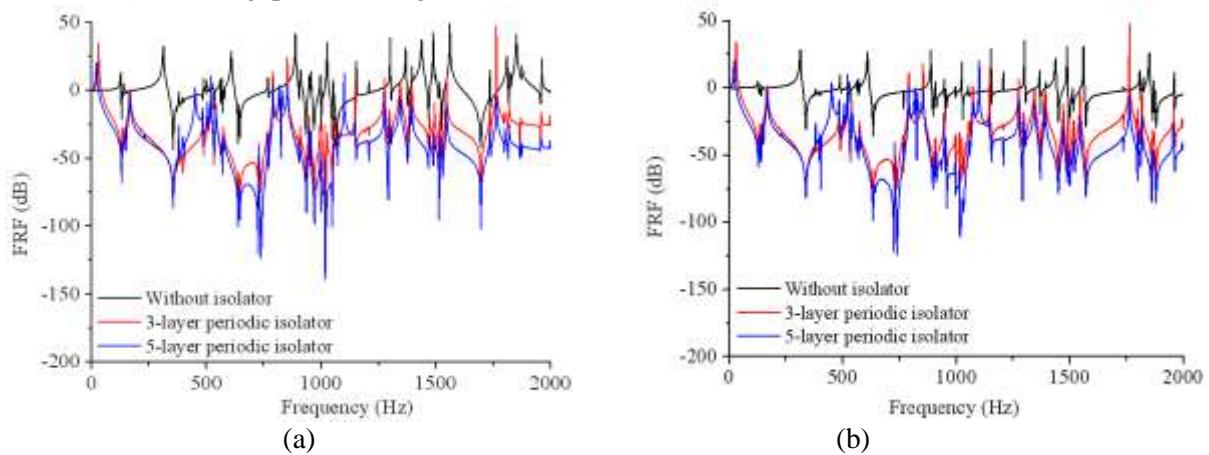**Fig. 6.**Band gaps of (a) longitudinal waves and (b) shear waves versus the filling ratio.

| (a) | (b) |

Fig. 8.FRFs ofnodes (a) N1 and (b) N10 under longitudinal waves.

| (a) | (b) |

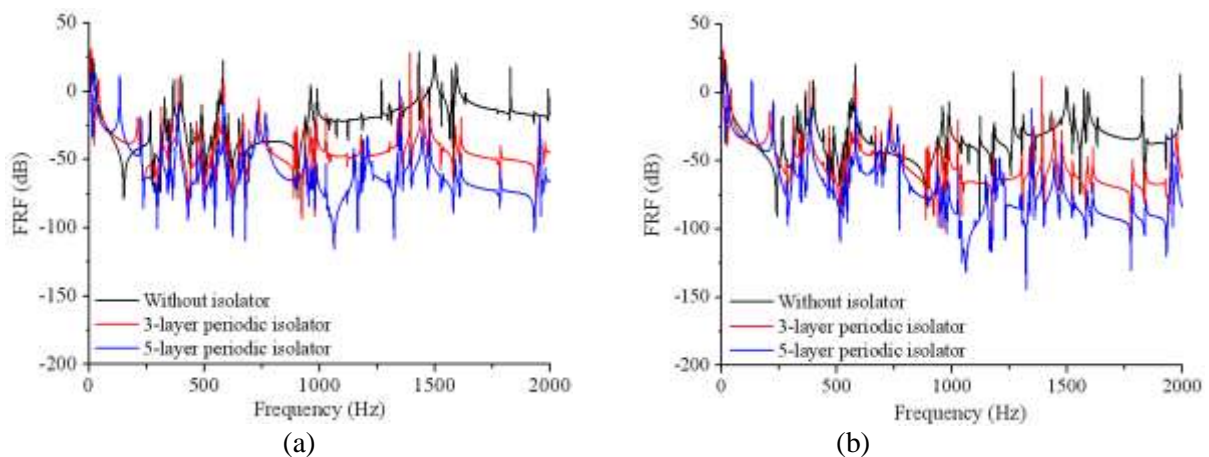**Fig. 9.**FRFs ofnodes (a) N1 and (b) N10 under shear waves in the *x*-direction.

(a)   (b)

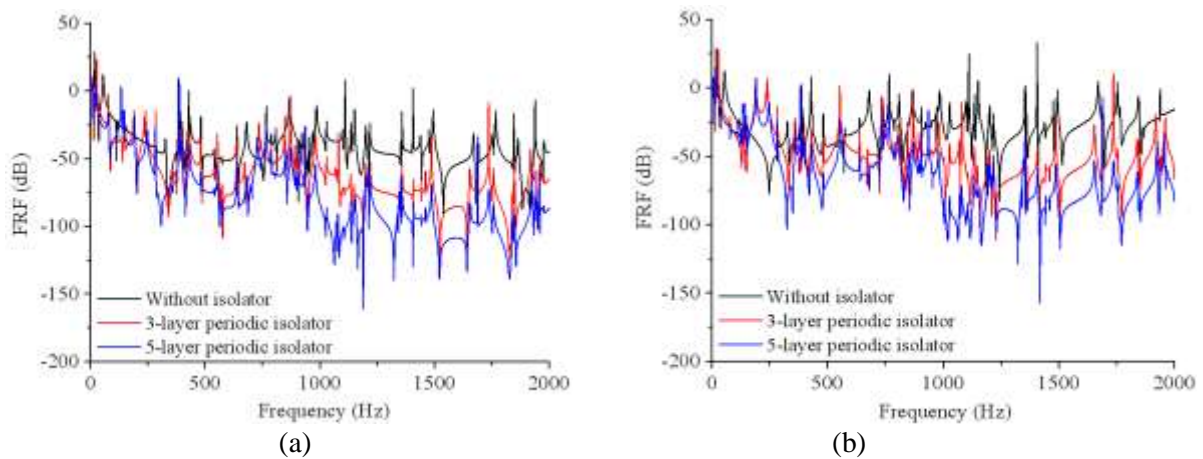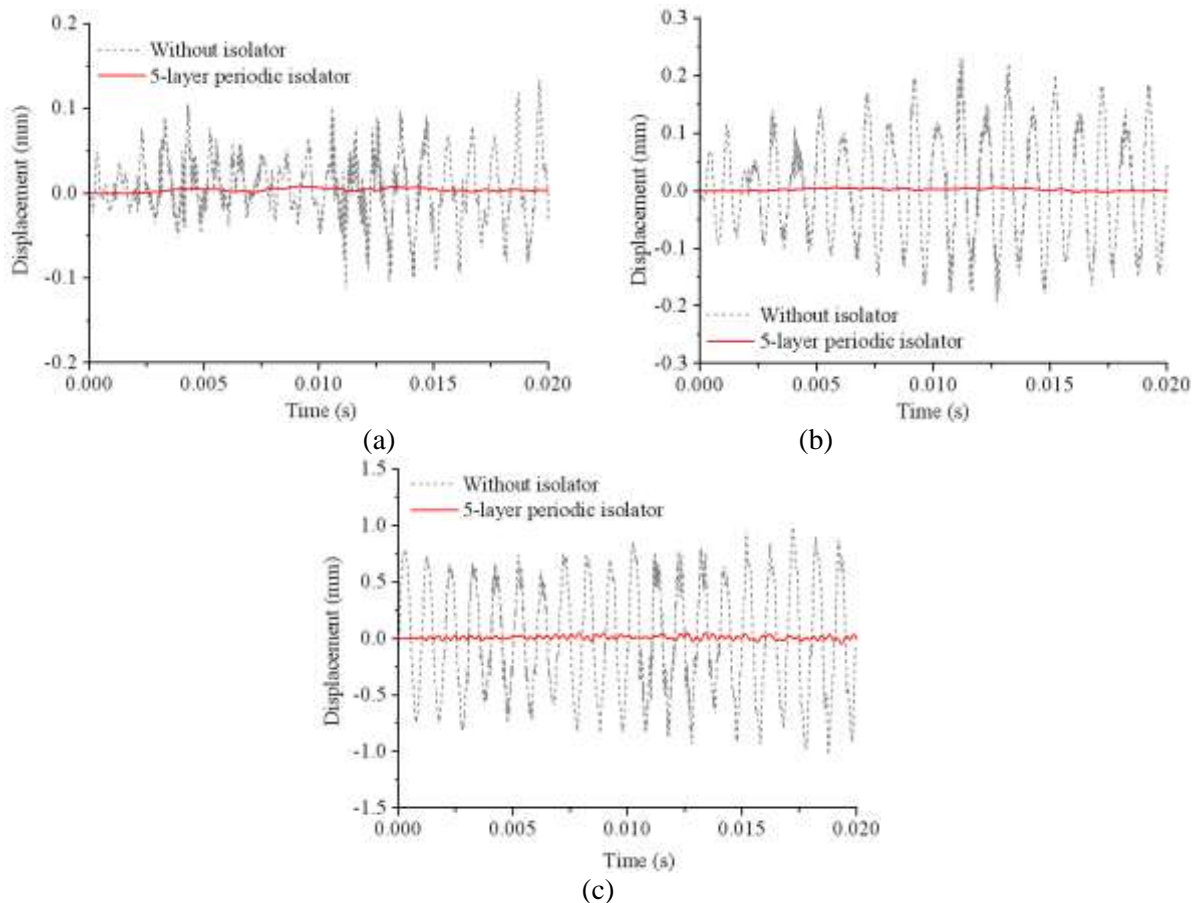**Fig. 10.** FRFs of (a) N1 and (b) N10 under shear waves in the *y*-direction.

(a)   (b)

(c)

Fig. 11. Dynamic response of N10 under harmonic excitation in the (a) *x*-, (b) *y*- and (c)*z*-directions
with *f*=1000 Hz.